Chemistry—Methods

Research Article
doi.org/10.1002/cmtd.202400067

Chemistry Europe
European Chemical
Societies Publishing

www.chemistrymethods.org

Raman Study of Intermediates Formed During the Electrochemical *N*-Nitrosation of Secondary Amines

Scott Richardson,[a] Rasool Babaahmadi,[b, c] Lee E. Edwards,[c] Rojan Ali,[c] Rebecca L. Melen,[b] Debdulal Roy,*[a] and Thomas Wirth*[c]

An *in situ* electrochemical Raman method is described to identify and validate the reaction pathway of amine nitrosations using density functional theory (DFT). In this reaction, sodium nitrite is used as an affordable and readily available nitrosating reagent, which also serves as an electrolyte in the reaction. This is a green approach towards nitrosations as it does not require the use of acids and other harsh or toxic solvents and chemicals. Intermediate species have been detected using Raman spectroscopy and are correlated with the calculated spectra expected in the reaction pathway to the *N*-nitrosamine products.

Introduction

N-Nitrosamines have often carcinogenic[1–4] and mutagenic properties, and can be found in the environment as contaminants in air, soil, water, drinks, drugs, and diet.[5,6] They originate from industrial chemical processes or from incomplete combustion. Therefore, detection and monitoring of those contaminants in a chemical process is highly important. This is to prevent their occurrence which may enter as impurities in products made for human consumption, such as pharmaceuticals. Dinitrogen tetroxide (N_2O_4) is a known reagent which can be generated *in situ* or utilised directly as NO_2 for the synthesis of *N*-nitrosamines.[7–15] Infrared (IR) spectroscopy has been used to study N_2O_4 and the presence of its different isomers.[16–24] Nitrogen oxides are known to be Raman active and have all been fully characterised using this technique. They can also be quantified in solutions provided the experiments are calibrated.[25–28] Electrochemical Raman spectroscopy can be used to study the nature of intermediates formed during an electrochemical reaction. The combination of cyclic voltammetry (CV) and electrochemical Raman spectroscopy could be a powerful tool providing a greater understanding of the redox reactions and the formation of intermediates occurring in nitrosations. With the combination of these techniques, it is possible to see structural changes in the compounds when a range of bias potentials and currents are applied. Cyclic voltammetry is unable to show structural changes alone, however, in combination with Raman spectroscopy this becomes possible. Vibrational Raman spectroscopy has the potential to reveal the identity of many different redox intermediates, although not surprisingly, the vibrational spectra from these experiments can be very complex due to the large number of possible products.

In this study, we focus on the spectroscopic investigation of the electrochemical nitrosation of amines in an aqueous acetonitrile solution. When the technique is refined in future studies, it will allow for the electrosynthesis, testing and characterisation of other similar compounds, including nitro derivatives.

Background and Experimental Setup

There are several studies of N_2O_4, N_2O_5 and their compounds in the gas and solid phase,[29,30] but there are only a few investigations that have dealt with these compounds in solution. Work by Brooksby and McQuillan[31] on $NaNO_2$ under methanolic non-aqueous conditions demonstrated the formation of electrochemical products that are different to those formed in other non-aqueous solvents. Infrared spectra show that methanol reacts directly with the electrooxidation products of nitrite, and the presence of water also influences the product formation indicating that the solvent plays an important role in determining the fate of the intermediates that are formed in the absence of water. The radical monomer $\cdot NO_2$ can dimerise and form N_2O_4 at temperatures below dinitrogen tetroxide's boiling point of 21.1 °C.[32] However, the enthalpy of the dissociation-association reaction ($\Delta_f H^o_{(g)} = 57.12$ kJ mol^{-1}) is in between that of a typical covalently bound molecule and a van der Waals complex, so this bond is relatively weak.[31–32] In addition to NO_2 and N_2O_4, the generation of N_2O_3, NO_3^-, NO, and NO^+ are also postulated from chemical reactions involving

[a] *Chemistry Department, Grove Extension, Swansea University, Swansea, Cymru/Wales, UK*

[b] *School of Chemistry, Cardiff Catalysis Institute, Translational Research Hub, Cardiff University, Cardiff, Cymru/Wales, UK*

[c] *School of Chemistry, Cardiff University, Cardiff, Cymru/Wales, UK*

Correspondence: *Prof. Debdulal Roy, Chemistry Department, Grove Extension, Swansea University, Swansea SA2 8PP, Cymru/Wales, UK.*
Email: deb.roy@swansea.ac.uk

Prof. Dr. Thomas Wirth, School of Chemistry, Cardiff University, Park Place, Main Building, Cardiff CF10 3AT, Cymru/Wales, UK.
*Email: wirth@cf.ac.uk*

Supporting Information for this article is available on the WWW under https://doi.org/10.1002/cmtd.202400067

Chemistry—Methods

Research Article
doi.org/10.1002/cmtd.202400067

Chemistry Europe
European Chemical
Societies Publishing

nitrite and its oxidation products.[33] Harrar *et al.* also studied solutions of N_2O_4 and N_2O_5 in anhydrous and aqueous nitric acid using Raman spectroscopy to gain a more detailed knowledge of the species present in these solutions and to assess the applicability of Raman spectroscopy as an analytical measurement technique (examples in supporting information S1, S2 and S3).[29,30] The spectra of solutions of N_2O_4 in HNO_3 displayed evidence of the presence of the associated species ($3NO^+ \cdot NO_3^-$), which had been identified previously in a solid compound.[34,35] The effects of water on the spectra of these solutions were examined as there is an incomplete knowledge of the association of the species and how these compounds may interact with the solvent. It was confirmed that the nitronium cation, NO_2^+ is the dominant species in solutions of N_2O_5 in anhydrous HNO_3, and the spectra of concentrated solutions of N_2O_5 exhibit a band that had not been reported previously; as Raman spectroscopy is the only technique that directly measures N_2O_5 and NO_2^+.[29,30] This weak band has been attributed to a second vibrational mode of the molecule indicating a nonlinear conformation of the NO_2^+ ion which suggests that it is strongly associated with other species in solution. As the nitronium cation is known to be the primary reactant in solutions of N_2O_5 in HNO_3, the intensity of its Raman band at 1400 cm^{-1} is a good indicator of its concentration.[29,30] The Raman data indicated that N_2O_5 in HNO_3 is completely ionised into NO_2^+ and NO_3^- (with a strong band at 1050 cm^{-1}) at concentrations up to at least 3 mol L^{-1} (21 wt%).[29,30] In solvents of high electrical conductivity, such as anhydrous HNO_3, N_2O_5 behaves as a strong electrolyte, and ionises to NO_2^+ and NO_3^-.[36] N_2O_4 also ionises to NO^+ and NO_3^- when dissolved in HNO_3 and there is evidence of the presence of an associated species ($3NO^+ \cdot NO_3^-$) in addition to the well-known nitrosonium cation, NO^+.

The equilibria in these solutions are strongly influenced by the concentration of water, because it influences the degree of dissociation of HNO_3 and hence the concentration of NO_3^- ion.[29,30]

Here we investigate the reaction between sodium nitrite and *N*-methylbenzylamine **1** as an exemplary secondary amine in 1:1 acetonitrile/water (Scheme 1). Masui and co-workers used this electrochemical approach with a different solvent system as a batch process towards the synthesis of *N*-nitrosamines with sodium nitrite as the nitrosating source,[13] while we have recently reported a flow electrochemical approach.[15]
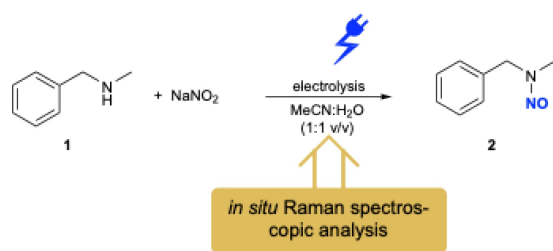
Conventional routes to *N*-nitrosamines involve the use of sodium nitrite in combination with a strong acid.[37–41]

The Raman instrumentation is shown in detail in the supporting information Figure S8. The experimental setup itself for the electrochemical Raman measurements uses a 3-electrode PEEK (polyether ether ketone) electrochemical cell setup (see supporting information, Figures S6 and S7). A graphite cross-section was used as the working electrode to determine the effect of the graphite surface area/topography on the reaction intermediates and products formed. A grub screw and a PTFE (polytetrafluoroethylene) holder are used to hold the graphite strip in place. With graphite acting as the anode and platinum as cathode in this setup, *N*-methylbenzylamine **1** is used for the electrolysis towards *N*-nitrosamine **2**. A potential window of 2.1 V was used throughout the reaction. The Raman microscope included a 488 nm excitation wavelength laser with 2.5 mW to the sample. A grating of 2400-line mm^{-1}, an Olympus Objective lens of 40× magnification with 0.5 NA, and an exposure time of 40 seconds. The electrochemical experiment was carried out at ambient temperature inside the cell. The Autolab potentiostat PGSTAT204 was used with a three-electrode set up and Raman spectra were acquired over a range of potentials that produce simultaneously the relevant CV curve and Raman spectra. The peaks on the Raman spectra over the potential range provide evidence to support the proposed intermediates and products formed during the course of the reaction. The Raman spectra measured the composition of the mixture of reactants, intermediates and products depicting presence of the species. It is limited by the sensitivity of the Raman signal from a specific species as intermediate concentrations are expected to be low and short lived. It is also limited by the time resolution for the intermediates that are short lived. For this reason, we considered a steady state where all the species are expected to be observed.

A 5 M aqueous sodium nitrite solution was added to the 1 M secondary amine dissolved in acetonitrile.[15] This is necessary for the reaction to proceed efficiently, and also to ensure good signal to noise from the Raman measurement. In this reaction the $NO_2^{\bullet}$ radicals not only dimerise but can also form various other species under the electrochemical conditions.[15] Both solutions are added to the cell and quickly mixed to create a homogeneous solution and the electrochemical Raman measurements started immediately. As the nitrite solution has sufficient conductivity, there is no need for any additional supporting electrolyte. In this setup, a one electron anodic oxidation of the nitrite ion provides the $NO_2^{\bullet}$ radicals, which exist in equilibrium with dinitrogen tetroxide (N_2O_4),[42] which is a known nitrosating agent for secondary amines under neutral or alkaline aqueous conditions and in organic media.[10] Raman spectra of the reagent solutions (a, b) and the spectrum of the *N*-nitrosamine **2** (c) are shown in Figure 1, Scheme1.
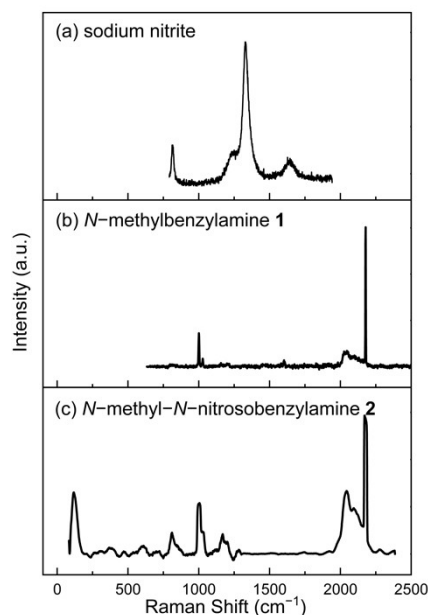

Scheme 1. *In situ* Raman analysis for the electrochemical synthesis of *N*-methyl-*N*-nitrosobenzylamine **2**.

Chemistry—Methods

Research Article
doi.org/10.1002/cmtd.202400067

Chemistry Europe
European Chemical
Societies Publishing

Figure 1. Raman spectra of a) sodium nitrite; b) *N*-methylbenzylamine **1**; c) *N*-methyl-*N*-nitrosobenzylamine **2**.

Results and Discussion

The reaction mechanism was investigated using a current-voltage CV measurement on the reaction mixture with an oxidation peak is observed around 0.4 V (vs Ag/AgCl) (see supporting information, Figure S4). A smaller oxidation peak is observed around 1.4 V. This result, in combination with past literature reports,[14,43,44] suggests a possible reaction mechanism shown in Figure 2. Initially, the NO_2^- anion undergoes a one electron oxidation to the $NO_2^\bullet$ radical. This species can dimerise to form N_2O_4, which is in equilibrium with a NO^+ cation and NO_3^- anion in solution. They interact with the amine **1** to form **add-1**, which is followed by the nitrosation (**add-2**) and an introduction of a hydroxide anion, generated from the reduction of water at the cathode. This resulting intermediate (**add-3**) allows the formation of the desired *N*-nitrosamine **2**, with the release of one water molecule and a nitrate anion.[13] In continuation of investigating our previously reported mechanism[15] using density functional theory (DFT) at the SMD/ωB97XD/def2tzvp//B3LYP-D3/6-31G(d) level, we replaced for the current study the symmetric secondary amine (dibenzylamine) with the asymmetric secondary amine **1**. The formation of **int-*cis*** and its conversion to **int-*trans*** as the active N_2O_4 isomers has already been discussed.[15] Figure 2 shows the calculated reaction pathway for the formation of *N*-nitrosamine product **2** from the reaction between **int-*trans*** and amine **1**.
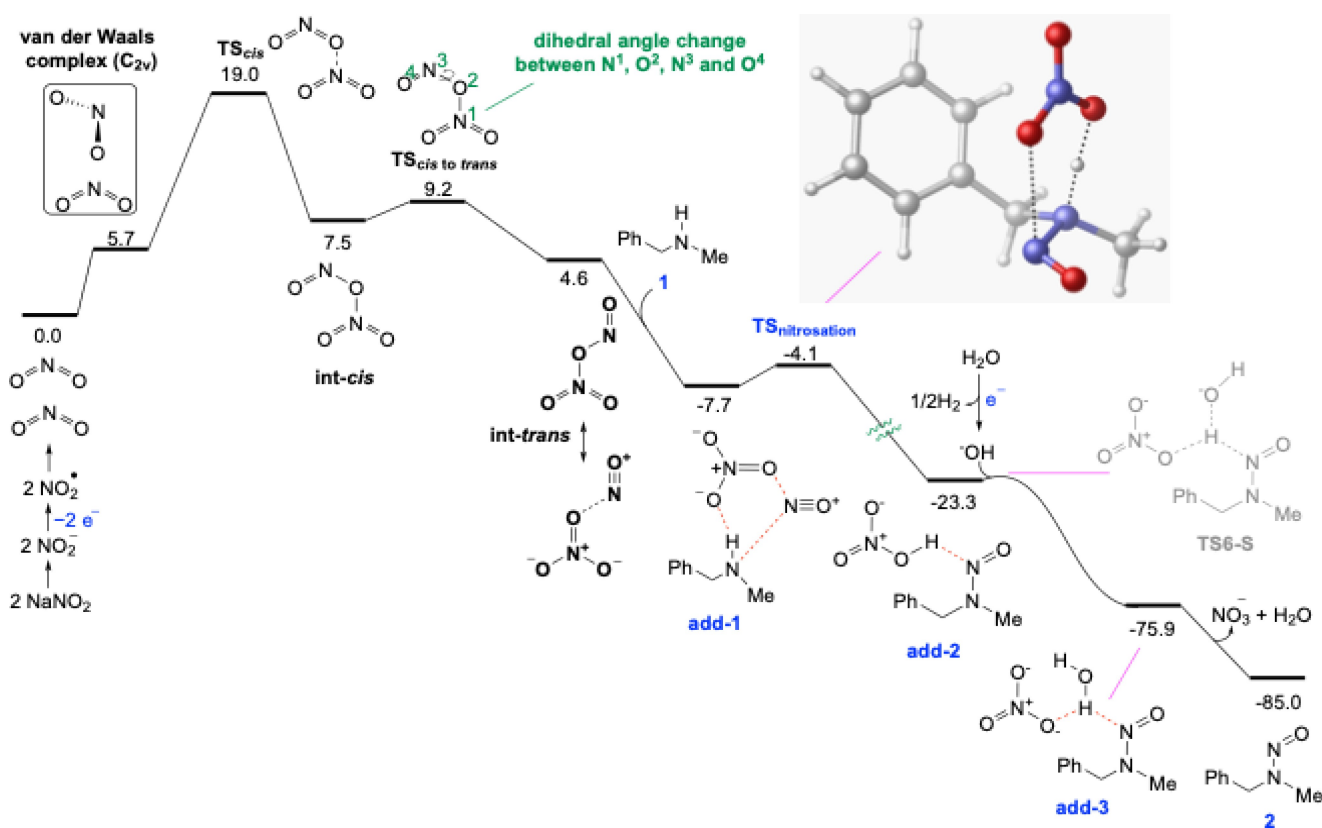

Figure 2. DFT calculated reaction pathway for the formation of *N*-nitrosamine **2** at the SMD/ωB97X-D/def2tzvp//B3LYP-D3/6-31G(d) level of theory. The relative free energies are given in kcal mol⁻¹.

Chemistry—Methods

Research Article
doi.org/10.1002/cmtd.202400067

Chemistry Europe
European Chemical
Societies Publishing

DFT calculated Raman spectra for each of the intermediate species formed during the reaction are shown in Figure 3. The stacked plots show the calculated spectra for the intermediates against the experimental spectra produced at a potential of 2.1 V. Vertical dashed lines are given for guidance to relate the calculated species and the experimental spectra to identify the intermediates contributing to the reactants and products formed. No peaks are observed above 2600 cm^{-1}.

The calculated Raman spectra should be treated as guidance only since the environment of the species are not the same in the experimental set up. It is expected that charge state of the molecule, laser wavelength dependence and the local environment influence the Raman spectra resulting in difference in relative intensities of the Raman peaks. Even with these limitations, it can be observed in Figure 3 that all species (**van der Waals complex**, **TS**$_{cis}$, **int-cis**, **TS**$_{cis\ to\ trans}$ and **int-trans**) are contributing to the product reaction pathway. Figure 3 shows the detection of **1**, **add-1**, **add-2**, **add-3** and product **2** confirming them as contributors. The pathway for the formation of final product **2** is occurring through the **int-cis** route and **int-trans** formation. In the process of NO$_2$ isomerisation, the formation of **int-cis** is kinetically preferred, with an activation barrier of 19.0 kcal mol^{-1}. Subsequently, **int-cis** can be converted to **int-trans** via a dihedral angle rotation, requiring a low activation barrier of just 1.7 kcal mol^{-1}. After **TS**$_{cis\ to\ trans}$, the intermolecular *N*-nitrosation of the secondary amine **1** progresses by forming adduct **add-1** and leading to the production of the final product *N*-nitrosamine **2**. The generation of adducts (**add-2** and **add-3**) also occurs through transition structure **TS**$_{nitrosation}$, which has an energy barrier of 3.6 kcal mol^{-1}.

When the theoretical spectra of **add-2** and **add-3** are plotted against the final product and the secondary amine, there is clearly a signal overlap that suggests these intermediates are present and are forming during the reaction. This is further illustrated in Figure 3 (magnified and clarified with peak assignments in supporting information Figures S9 and S10). The HNO$_3$ species is contributing to the reaction as nitric acid can be formed from the by-products NO$_3^-$ and H$_2$O as part of the breakdown of **add-3** to product **2** in the reaction pathway. The assignment of the Raman peaks is summarised in Table 1.

Conclusions

A combination of the applied potential, in this case 2.1 V for optimum reaction conditions, and the graphite electrode surface is enabling the electron transfer to take place during the reaction. Furthermore, it can be concluded that electrochemical Raman techniques in combination with DFT calculations can be used in the identification of intermediates during a reaction exemplified with a nitrosation reaction.

With sodium nitrite as the nitrosating source, the non-hazardous, straightforward, and simple experimental approach avoids the use of additional supporting electrolytes or other toxic reagents. Additionally, ambient temperatures and less hazardous solvents were employed for this reaction avoiding harsh reaction conditions.
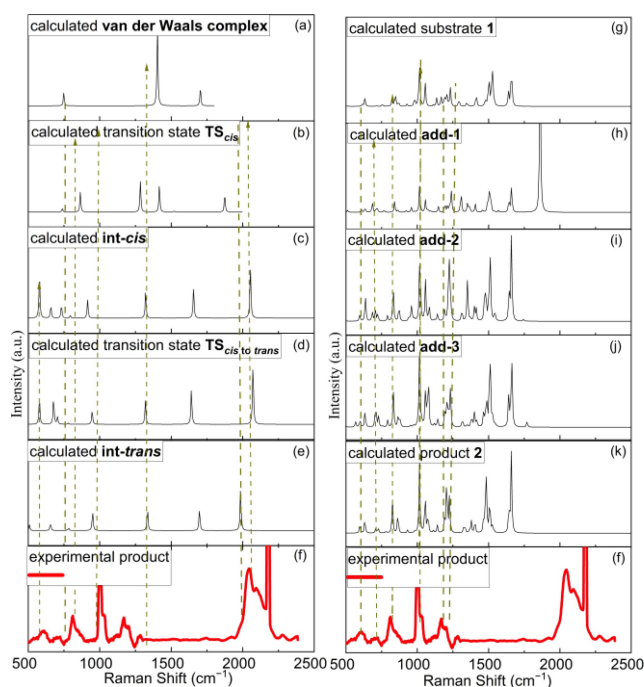
Figure 3. Raman spectra of the calculated spectra (a–e, g–k) of the compounds detected from data processed against the final experimental product spectra (f) taken at 2.1 V. Dashed lines are given as guidance to relate the intermediate species appearing in the reaction pathway.

Table 1. Assignment of Raman peaks from experimental and calculated Raman spectra.

Entry	Wavenumber (cm^{-1})	Peak assignments
1	110	van der Waals complex
2	850	**TS**$_{cis}$
3	603	**int-cis**
4	603, 2062	**TS**$_{cis\ to\ trans}$
5	2022	**int-trans**
6	612, 820, 997, 1173, 1205	substrate **1**
7	820, 997, 1173, 1205	**add-1**
8	612, 820, 997, 1173, 1205	**add-2**
9	612, 820, 997, 1173, 1205	**add-3**
10	612, 820, 997, 1173, 1205	product **2**

Chemistry—Methods

Research Article
doi.org/10.1002/cmtd.202400067

Chemistry
Europe
European Chemical
Societies Publishing

Conflict of Interests

The authors declare no conflict of interest.

Data Availability Statement

The data that support the findings of this study are available in the supplementary material of this article.

[1] P. N. Magee, J. M. Barnes, *Br. J. Cancer* **1956**, *10*, 114–122.
[2] W. Lijinsky, *Cancer Metastasis Rev.* **1987**, *6*, 301–356.
[3] Y. L. Kostyukovskii, D. B. Melamed, *Russ. Chem. Rev.* **1988**, *57*, 350–366.
[4] A. R. Tricker, R. Preussmann, *Mutat. Res.* **1991**, *259*, 277–289.
[5] J. B. Guttenplan, *Mutat. Res. Genet. Toxicol.* **1987**, *186*, 81–134.
[6] W. Jin-Mei, L.-S. Shoei-Yn, L. Jen-Kun, *Biochem. Pharmacol.* **1993**, *45*, 819–825.
[7] E. H. White, W. R. Feldman, *J. Am. Chem. Soc.* **1957**, *79*, 5832–5833.
[8] D. J. Lovejoy, A. J. Vosper, *J. Chem. Soc. Inorg. Phys. Theor.* **1968**, 2325–2328.
[9] B. C. Challis, S. A. Kyrtopoulos, *J. Chem. Soc. Chem. Commun.* **1976**, 877–878.
[10] B. C. Challis, S. A. Kyrtopoulos, *J. Chem. Soc. Perkin Trans. 2* **1978**, 1296–1302.
[11] B. C. Challis, S. A. Kyrtopoulos, *J. Chem. Soc. Perkin Trans. 1* **1979**, 299–304.
[12] M. Nakajima, J. C. Warner, J.-P. Anselme, *Tetrahedron Lett.* **1984**, *25*, 2619–2622.
[13] M. Masui, N. Yamawaki, H. Ohmori, *Chem. Pharm. Bull.* **1988**, *36*, 459–461.
[14] Y. Wang, S. You, M. Ruan, F. Wang, C. Ma, C. Lu, G. Yang, Z. Chen, M. Gao, *Eur. J. Org. Chem.* **2021**, 3289–3293.
[15] R. Ali, R. Babaahmadi, M. Didsbury, R. Stephens, R. L. Melen, T. Wirth, *Chem. Eur. J.* **2023**, *29*, e202300957.
[16] S. F. Agnew, B. I. Swanson, L. H. Jones, R. L. Mills, *J. Phys. Chem.* **1985**, *89*, 1678–1682.
[17] L. H. Jones, B. I. Swanson, S. F. Agnew, *J. Chem. Phys.* **1985**, *82*, 4389–4390.
[18] A. Givan, A. Loewenschuss, *J. Chem. Phys.* **1989**, *90*, 6135–6142.
[19] A. Givan, A. Loewenschuss, *J. Chem. Phys.* **1989**, *91*, 5126–5127.
[20] A. Givan, A. Loewenschuss, *J. Chem. Phys.* **1991**, *94*, 7562–756.
[21] W. G. Fateley, H. A. Bent, B. Crawford, *J. Chem. Phys.* **1959**, *31*, 204–217.
[22] I. C. Hisatsune, J. P. Devlin, Y. Wada, *J. Chem. Phys.* **1960**, *33*, 714–719.
[23] R. V. St. Louis, B. Crawford, *J. Chem. Phys.* **1965**, *42*, 857–864.
[24] H. Beckers, X. Zeng, H. Willner, *Chem. Eur. J.* **2010**, *16*, 1506–1520.
[25] J. E. Harrar, R. K. Pearson, *J. Electrochem. Soc.* **1983**, *130*, 108–112.
[26] J. A. Happe, A. G. Whittaker, *J. Chem. Phys.* **1959**, *30*, 417–421.
[27] C. C. Addison, *Chem. Rev.* **1980**, *80*, 21–39.
[28] J. E. Harrar, R. Quong, L. P. Rigdon, R. R. McGuire, *J. Electrochem. Soc.* **1997**, *144*, 2032–2044.
[29] J. E. Harrar, L. P. Rigdon, S. F. Rice, *J. Raman Spectrosc.* **1997**, *28*, 891–899.
[30] J. E. Harrar, R. K. Pearson, *J. Electrochem. Soc.* **1983**, *130*, 108–112.
[31] P. A. Brooksby, A. J. McQuillan, *J. Phys. Chem. C* **2010**, *114*, 17604–17609.
[32] CRC Handbook of Chemistry and Physics, 73rd edn. Boca Raton, Florida, CRC Press 1992–1993.
[33] M. W. Chase, *J. Phys. Chem. Ref. Data* **1998**, *9*, 1529–1564.
[34] C. C. Addison, L. J. Blackwell, B. Harrison, D. H. Jones, N. Logan, E. K. Nunn, S. C. Wallwork, *J. Chem. Soc. Chem. Commun.* **1973**, 347–348.
[35] L. J. Blackwell, E. K. Nunn, S. C. Wallwork, *J. Chem. Soc. Dalton Trans.* **1975**, 2068–2072.
[36] N. Logan, *Pure Appl. Chem.* **1986**, *58*, 1147–1152.
[37] A. B. L. Fridman, F. Mukhametshin, S. S. Novikov, *Russ. Chem. Rev.* **1971**, *40*, 34–50.
[38] K. Kano, J. P. Anselme, *Bull. Soc. Chim. Belg.* **1983**, *92*, 229–232.
[39] V. E. Platonov, A. Haas, M. Schelvis, M. Lieb, K. V. Dvornikova, O. I. Osina, T. V. Rybalova, Y. V. Gatilov, *J. Fluorine Chem.* **2002**, *114*, 55–61.
[40] K. Laihia, A. Puszko, E. Kolehmainen, J. Lorenc, *J. Mol. Struct.* **2007**, *831*, 203–208.
[41] A. Klasek, A. Lyčka, F. Křemen, A. Růžička, M. Rouchal, *Helv. Chim. Acta* **2016**, *99*, 50–62.
[42] C. E. Castellano, A. J. Calandra, A. J. Arvia, *Electrochim. Acta* **1974**, *19*, 701–712.
[43] C. Castellano, J. Wargon, A. Arvia, *J. Electroanal. Chem. Interfacial Electrochem.* **1973**, *47*, 371–372.
[44] N. Tanaka, K. Kato, *Bull. Chem. Soc. Jpn.* **1956**, *29*, 837–842.